

Contactless Switching of a RF CBRAM Switch

Daisuke Kobuchi⁽¹⁾, Romain Siragusa⁽²⁾, Yoshiaki Narusue⁽¹⁾, Arnaud Vena⁽³⁾, and Etienne Perret⁽²⁾

(1) Graduate School of Engineering, The University of Tokyo, Tokyo, Japan; e-mail: {kob, narusue}@mlab.t.u-tokyo.ac.jp

(2) LCIS, Grenoble Institute of Technology, Valence, France; e-mail: {etienne.perret, romain.siragusa}@lcis.grenoble-inp.fr

(3) University of Montpellier, Montpellier, France; e-mail: arnaud.vena@umontpellier.fr

Abstract

This paper proposes a method to wirelessly rewrite the CBRAM switches for chipless RFID tag IDs. The contactless driving of the CBRAM switch is achieved by inductive coupling between a writer coil and a tag coil. On the writer side, a voltage pulse is generated on a coil which induces a varying electromotive force across another coil which is connected to the CBRAM (device part). Numerical analysis and circuit simulations were performed to confirm that pulse waves are thus induced in the device coil and it allows to switch the CBRAM. In addition, experimental results showed that the CBRAM was successfully switched from the On state to the Off state by applying multiple pulses to the writer coil.

1 Introduction

In recent years, with the increase in Internet-of-things (IoT) devices and the proliferation of Radio-frequency identification (RFID) barcodes, a lot of research and development on chipless RFID has been conducted [1]. Chipless RFID is based on the principle of backscattering communication technique. Like the barcode, the information is contained in the shape of the pattern printed on a label with the difference that these patterns must be conductive. Based on a radar principle operated in RF, it is the wave backscattered by the label that contains the ID of the tag and which, once recovered by the reader, will be analysed to trace the tag ID. Chipless RFID is essentially low-cost because it does not require a chip and can be manufactured using only a printing process. Therefore, chipless RFID is suitable for applications that use a large number of tags, such as barcodes and IoT devices.

On the other hand, conventional chipless RFID has a limitation because once the tag is printed, the information is written into the tag and it cannot be rewritten after manufacturing. Therefore, like for the barcodes, if the tag information needs to be changed, another chipless RFID has to be manufactured. The ability to modify the tag information with a write, rewrite function is something that has been awaited over the past decade and would significantly increase the life of the tags while reducing the environmental impact. Therefore, the concept of a rewritable chipless

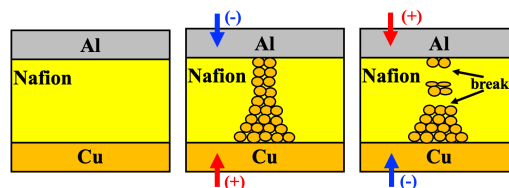


Figure 1. Structure of CBRAM and filament formation controlled by voltage.

tag has been introduced [2]. The challenge here is to have a RF switch that controls the tag ID, without any chips, batteries or electronic components. CBRAM technology was used to make the very first rewritable chipless tags. Then, rewritable chipless RFID tags operating up to 10 GHz have been introduced [3]. In addition, 25 cycles of On/Off state have been reached and these switches have also been integrated in filters and antennas to increase their functionalities [2]. However, the CBRAM's electrodes have to be in contact to DC probes when writing, which is costly, and the electrodes get deteriorated due to the contact. In addition, when a rectangular loop scatterer is used to encode the ID, the conventional writing method using probes required cutting the metallic loop to prevent DC short-circuit issue during writing [2].

For all these reasons, a contactless solution would greatly facilitate the development of the rewritable chipless RFID. Therefore, contactless writing of chipless RFID tag is proposed in this study. This is achieved by inducing multiple pulses into the CBRAM with the use of two inductively coupled coils. By using short pulses, contactless writing can be achieved without connecting the CBRAM electrode to a signal generator and without cutting the scatterer. In section II, the basic principle of rewritable chipless RFID using CBRAM is explained. A novel writing method of CBRAM is proposed in section III and the experimental results are shown in section IV. Finally, a conclusion is presented in section V.

2 Rewritable Chipless RFID based on CBRAM

CBRAM is a technology used in resistive memory [4] and the stacking of layers used in this study is shown in Fig. 1. In general, CBRAM has two electrodes made of inert and

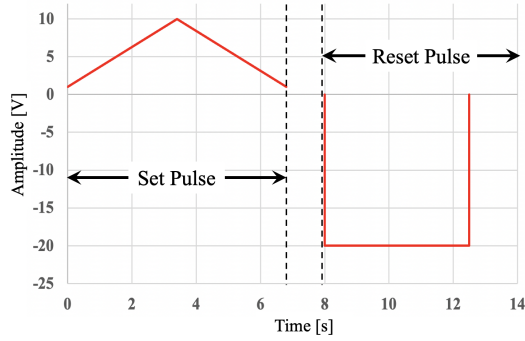


Figure 2. Direct current (DC) pulses used with CBRAM cells in a classical writing method [5].

active metal. In this study, the 2-dimensional implementation is made with two electrodes : one active in copper and one inert in aluminium. Between the two electrodes, Nafion is inserted as an ion conductive layer. When a positive voltage is applied to the active electrode, some ions Cu^+ are detached from the Cu electrode and migrate toward the Al electrode. Once arrived at the level of the aluminum electrode, the Cu^+ ions are reduced which gradually forms a copper filament. Once this conductive filament connects the two electrodes, the CBRAM becomes in the On state, describing a conducting state with a very low resistance. On the other hand, when a negative voltage is applied, the filament is broken, forming an open state, and the resistance of the CBRAM increases. When the two electrodes are connected directly to DC probes [2, 3], the signal generated to switch On the CBRAM cell is typically a continuous ramp voltage from 0 V to 10 V. On the contrary, to switch Off the CBRAM, DC voltage around -20 V was used. Fig. 2 shows the evolution in time of these two signals used so far to control the state of the switch.

In this research, a contactless switching of CBRAM switch is proposed and the configuration of the writing circuit is shown in Fig. 3(a). We note that trying to switch the CBRAM cell remotely completely modifies the control signals, in fact it is no longer possible to use DC signals like those shown in Fig. 2. Indeed, it is not possible to impose this same type of voltage in a non-contact way, at best it is possible to send short voltage pulses through inductive coupling to achieve the control of the switch. This demonstration is at the heart of this paper, where the objective is to show a new approach to remotely control a CBRAM. Therefore, we focused on the use of a set of pulses to switch the CBRAM.

3 Principle of contactless writing with pulses

To validate the proposed approach, a numerical analysis has first been conducted. Then, circuit simulations were done using a full wave EM simulator.

3.1 Numerical analysis

With the two coupled coils shown in Fig. 3, the circuit equation can be expressed in terms of differential equations

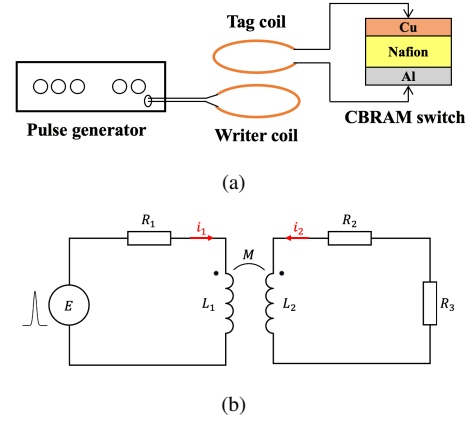


Figure 3. (a) Proposed writing circuit. (b) Equivalent circuit of the writing circuit.

Table 1. Parameters of the circuit

Parameters	Value [mm]
R_1, R_2, R_3	$8.8e-6, 8.8e-6, 50 [\Omega]$
L_1, L_2	$79.4, 79.4 [\text{nH}]$
M	$60.2 [\text{nH}]$
Width of pulse	$65 [\text{ps}]$
Amplitude of pulse	$6 [\text{V}]$

as follows:

$$\begin{cases} R_1 i_1 + L_1 \frac{di_1}{dt} + M \frac{di_2}{dt} = E(t) \\ (R_2 + R_3) i_2 + L_2 \frac{di_2}{dt} + M \frac{di_1}{dt} = 0. \end{cases} \quad (1)$$

In (1), i_1 and i_2 are the current at the writer coil and the tag coil. R_1 and R_2 are the resistances of the writer coil and the tag coil. R_3 is the resistance of the CBRAM. L_1 and L_2 are the self inductances of the writer coil and the tag coil. M is the mutual inductance between the writer coil and the tag coil. $E(t)$ is the pulse-wave voltage. Since it is difficult to solve (1) analytically, they were solved numerically. Initial conditions and various parameters are set as shown in the Table 1.

To obtain the values of the parameters given in Table 1, a first simulation on an electromagnetic solver (CST Magnetostatic Solver) was performed. A coil radius of 16 mm, wire diameter of 0.5 mm and a distance between the two coils of 0.5 mm have been considered in the simulation as seen in Fig. 4. The number of turns at the tag and the writer is limited to 1 to be able to implement the coil on a single layer printed circuit board in the future, i.e. a configuration compatible with the manufacture of a chipless tag. The resistances of coils, R_1 and R_2 have been derived by $\rho l/A$, where ρ is electrical resistivity of copper, l is the length of a coil and A is the cross-sectional area of a coil. The inductances, L_1 and L_2 and the mutual inductance, M are calculated by the electromagnetic simulator. With these values, the differential equations (1) were solved numerically with Mathematica and the result is shown in Fig. 5.

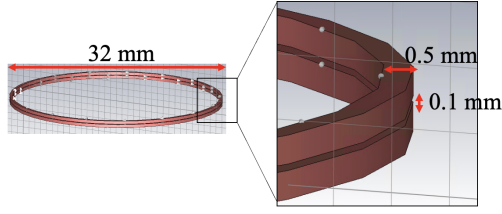


Figure 4. Coil models in CST.

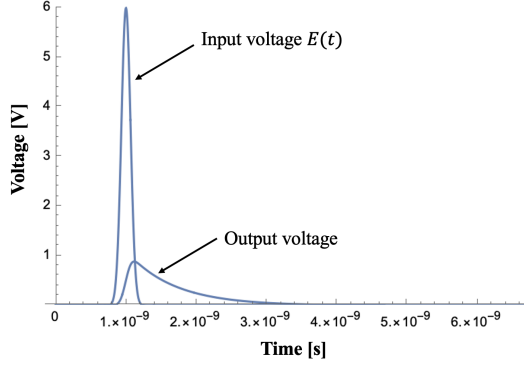


Figure 5. Simulation from (1) of the voltage at the terminals of the tag coil (Output voltage) when a pulse (Input voltage $E(t)$) is applied to the writer coil (cf. Fig.3).

This result shows that a positive pulse voltage is induced at the CBRAM terminals when a positive pulse voltage is applied at the writer coil. This indicates the possibility of obtaining a voltage of the order of 1 V on the CBRAM side and therefore potentially being able to change its state.

3.2 Full wave simulation

Although the differential equations assumed that the coil parameters were constant and independent of frequency, this is quite far from practice. In fact, they depend on frequency because parasitic capacitors at the coils exist and skin depth resistance values also depend on the frequency. Furthermore, input pulse waves occupy a wide frequency band and are therefore affected by frequency characteristics of the coils. To evaluate the induced voltage including the effect of the frequency dependences, the writer coil and the CBRAM coil were designed on the electromagnetic simulator FEKO using the same parameters of the coils shown in Fig. 4. FEKO is based on the method of moments (MoM), and s2p from 100 kHz to 10 GHz was extracted from the simulations.

The S matrix thus obtained as a function of frequency was used in a temporal solver in order to consider a pulse excitation and to simulate the induced voltage at the CBRAM in order to compare these results with those of section 3.1. The pulse excitation was calculated by a circuit simulator in CST using the S matrix file extracted from VNA measurement. The results are shown in Fig. 6. This results show that the voltage induced at the CBRAM terminals oscillates compared to the results obtained in section 3.1 where constant parameters in frequency were considered. However,

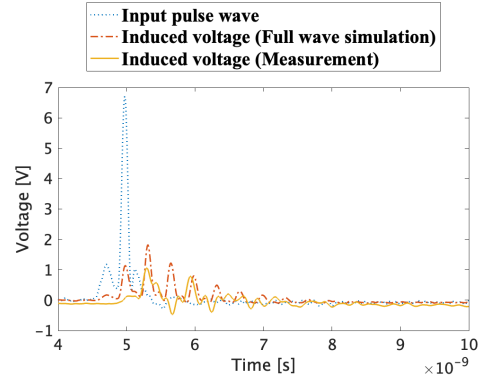


Figure 6. Input pulse voltage and induced voltage using simulated s2p and measured s2p.

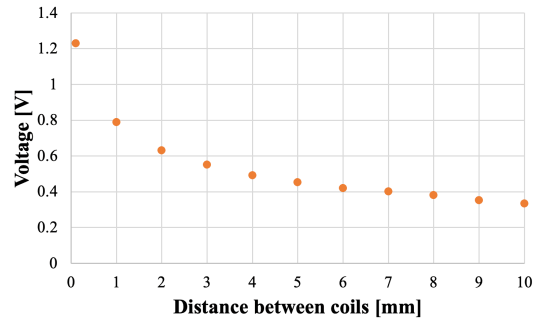


Figure 7. Peak of the induced voltage (CBRAM terminal) when changing the distance between coils.

a pulse voltage with the same sign as the input voltage is obtained on the CBRAM side with a magnitude of about 1 V. Fig. 7 shows the peak of the induced voltage when changing the distance between the writer coil and the tag coil. From this graph, it can be seen that the closer the distance, the higher the induced voltage is.

4 Measurement Results

4.1 Measurements of the induced voltage

Before the experiment using a CBRAM cell, S-parameters of the two coils (the 2 ports device shown in Fig. 8) have been measured with a network analyzer, FieldFox N9918A, Keysight from 100 kHz to 10 GHz. In parallel as previously explained, the output of a pulse generator, Model 3500D, Picosecond Pulse Labs has been measured with a 12-GHz band oscilloscope, DSO91204A, Keysight. With the S-parameters and the measurement in time of the pulse generator, the induced voltage at the CBRAM terminal have been obtained with FEKO has explained in section 3.2. A equivalent CBRAM resistance value of 50 ohm has been considered. The obtained results are shown in Fig. 6. Although the induced wave in the measurements is different from that obtained in full simulation, the absolute value of the positive peak is higher than that of the negative one.

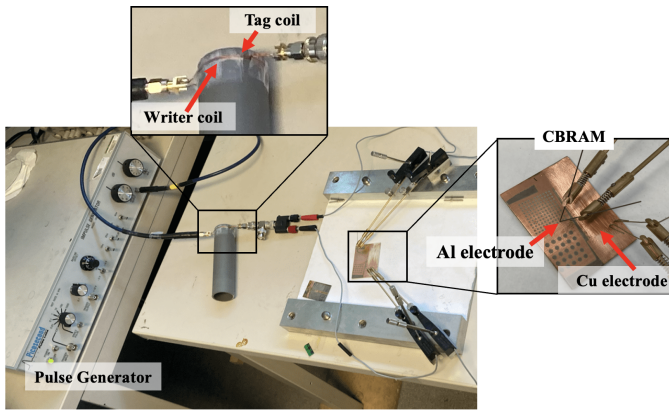


Figure 8. Experimental environment with implemented coils and CBRAM.

4.2 Contactless switching of CBRAM

To verify whether the contactless switching of CBRAM is possible, experiments are conducted with the pulse generator. This pulse generator is capable of generating pulses width of 65 ps and it was set to generate 1000 pulses per second. The pulse generator was connected to the writer coil to induce a pulse voltage at the CBRAM as shown in Fig. 8. In the experiments, the resistance of the CBRAM switch was measured with a source meter, Keithley, Model 2450 to confirm whether it is turned Off with pulses input to the writer coil. The pulse generator, writer coil, tag coil, and CBRAM were connected as shown in Fig. 8. The coils were made by winding wire around a cylinder with a radius of 16 mm and a wire diameter was 0.5 mm as shown in Fig. 8. The distance between the coils is a few hundreds of μm . The CBRAM used in the experiments is shown in Fig. 8. The CBRAM was made of a copper/Nafion/Al structure as shown in Fig. 1, with 600-nm thickness of Nafion and 500-nm thickness of aluminum stacked on a RO4003 substrate.

After it was confirmed that the CBRAM switch was turned Off, a ramp voltage as shown in Fig. 2 was applied to the CBRAM to turn it On again. On the other hand, the transition from the On to the Off state is carried out using the contactless method induced here, namely the use of pulses. This cycle Off to On (with voltage ramp) and On to OFF (with pulses) was repeated three times, with pulses output from the pulse generator for 60 seconds each time. The result of the experiments is shown in Fig. 9. This result shows that the resistance of the CBRAM is clearly increased by the pulse waveform. This indicates that the CBRAM was switched from the On state to the Off state by the pulse waveform, which means that the CBRAM on the tag can be switched Off wirelessly.

5 Conclusion

In this study, we solved the problem that CBRAM RF switches used in rewritable chipless RFID can only be rewritten by electrode contact. When contactless rewriting

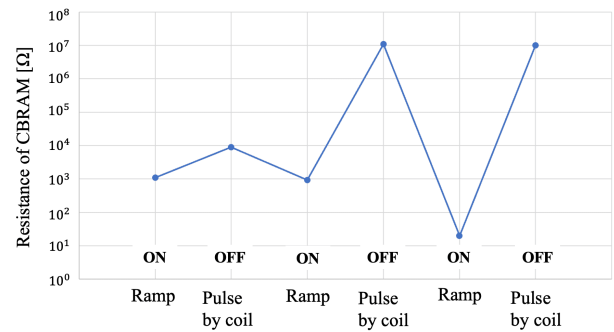


Figure 9. Switching results of CBRAM with pulse waves.

can be achieved, the cost of writing and the risk of damage of the tag can be reduced. The proposed method solved is based on the use of two coupled coils and an ultra short pulse excitation. First, we confirmed by numerical analysis and circuit simulation that a pulse-shaped induced voltage can be generated at the CBRAM terminals when a Gaussian pulse is input to the writer coil. Then, we experimentally confirmed that the CBRAM can be switched from the On state to the Off state by inputting a pulse voltage to the writer coil multiple times with a pulse generator. In the future, we plan to confirm the contactless switching of the CBRAM from the On state to the Off state.

Acknowledgements

This study was supported by JSPS KAKENHI Grant Numbers JP22J14609. This study was also supported by the European Research Council (ERC) through the European Union's Horizon 2020 Research and Innovation Program under Agreement 772539 (SCATTERERID).

References

- [1] E. Perret, "Radio Frequency Identification and Sensors: From RFID to Chipless RFID," *John Wiley & Sons - ISTE*, 2014.
- [2] J. M. Purushothama, S. Lopez-Soriano, A. Vena, B. Sorli, I. Susanti and E. Perret, "Electronically Rewritable Chipless RFID Tags Fabricated Through Thermal Transfer Printing on Flexible PET Substrates," *IEEE Transactions on Antennas and Propagation*, **69**, 4, pp. 1908–1921, April 2021.
- [3] A. Vena, E. Perret, S. Tedjini, C. Vallée, P. Gonon and C. Mannequin, "A fully passive RF switch based on nanometric conductive bridge," *2012 IEEE/MTT-S International Microwave Symposium Digest*, pp. 1–3, Montreal, QC, Canada, June 2012.
- [4] S. Dietrich et al., "A Nonvolatile 2-Mbit CBRAM Memory Core Featuring Advanced Read and Program Control," *IEEE Journal of Solid-State Circuits*, **42**, 4, pp. 839–845, April 2007.
- [5] J. M. Purushothama, A. Vena, B. Sorli, and E. Perret, "Electronically Re-Configurable, Non-Volatile, Nano-Ionics-Based RF-Switch on Paper Substrate for Chipless RFID Applications," *Technologies*, **6**, 3, p. 58, June 2018.